

# Detection of Buried and Partially Buried Objects Using A Bio-inspired Wideband Sonar

Chris Capus, Yan Pailhas, Keith Brown, David Lane  
Ocean Systems Laboratory, Heriot-Watt University, Edinburgh, Scotland, UK EH14 4AS  
<http://osl.eps.hw.ac.uk/>  
C.Capus@hw.ac.uk

**Abstract** - The Ocean Systems Laboratory is developing bio-inspired wideband acoustic sensing methods for underwater target detection and tracking. The wideband sensors themselves are based on bottlenose dolphin sonar, covering a frequency band from around 30kHz to 150kHz and having a frequency dependent beamwidth considerably larger than conventional imaging sonars. The entire system is relatively compact and is suitable for mounting on a variety of platforms including small scale autonomous underwater vehicles (AUVs). In this paper we overview recent efforts applying the sonar to the detection and tracking of various underwater cables, and to the detection and classification of these cables in shallow burial, based on their midwater responses.

## I. INTRODUCTION

The excellent performance of cetaceans in target detection and recognition has been intensively studied with increasing interest in recent years in the development of biomimetic sonar systems to further investigate and attempt to replicate some of these capabilities [1, 2]. The Ocean Systems Laboratory (OSL) is developing a bio-inspired wideband acoustic sensing system for autonomous underwater vehicles (AUVs) for improved detection and recognition of subsea objects [3]. One application for the new system is the autonomous tracking of underwater cables. The bio-inspired approach offers potential for cable recognition as well as improved detection, making tracking more robust in cluttered environments. This paper covers proof-of-concept research providing results of experiments in which the bio-inspired system has been tested against a number of different cables under various test conditions. These experiments aim to demonstrate the validity of the wideband approach in cable recognition and to explore the impact of reverberation and consistency of cable responses measured against different background sediments. The sensors themselves are based on bottlenose dolphin (*Tursiops truncatus*) sonar, covering a frequency band between 30-130kHz and having a frequency dependent beam width considerably wider than conventional imaging sonars, varying from around 40 at the highest frequency to around 80 at the lower end. We aim to use bio-inspired pulses to elicit characteristic wideband signatures to distinguish between different cable types. Data gathered from sample cables demonstrate an excellent capability for differentiation between different cable types and between cables and clutter objects and importantly the ability to detect and identify cables of around 25mm diameter and less.

## A. Cables

Four different cables, designated types A–D, have been studied during the experimental programme, with differences in construction for types A–C illustrated in Figure 1. The external diameters of the cables were between 16.5mm and 32mm. The type D cable is similar to type A but with a fibre optic core. All of the cables have a number of steel strands for strength with configurations varying between types.

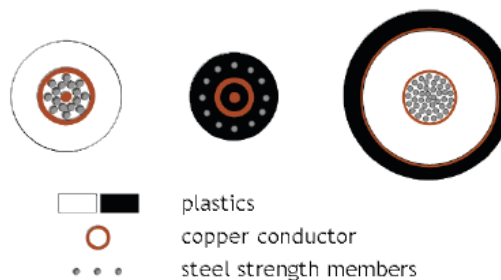


Figure 1: Cross sections of cable types under test.

## B. Experimental Setup

The test tank experimental set up is illustrated in Figure 2. Responses have been measured midwater and against two different sediment backgrounds, very fine sand and a coarse sand/grit mixture. For the midwater experiments, cable aspect was varied in the horizontal plane using a Bowtech PT-25 pan-and-tilt unit. Wideband high and low frequency projectors were tested with a matched pair of receivers mounted on a PT-10 pan-and-tilt unit. The sensor configuration used in these experiments is suitable for vehicle mounting in conjunction with a sidescan sonar and can be readily adapted to run alongside video or other sensors.

## C. Sensors and Signals

The OSL wideband sensors, developed by PCT Ltd from our own specifications, provide two projectors each covering around two octaves. The higher frequency unit has a peak response around 100kHz and -3dB band centre at around 100kHz. The lower frequency projector has a similar level peak response at approximately 85kHz with the -3dB band centred around 65kHz. In conjunction these sensors are capable of emitting significant energy in a band ranging from around 30kHz to nearly 200kHz. The cable cross-sections

present relatively small targets and in most tests the high frequency projector has proved most capable. The lower frequency unit may still find application in situations where cable burial is a problem.

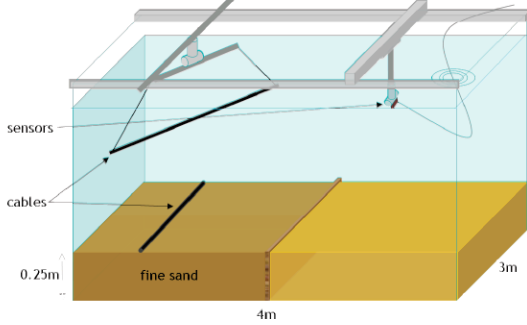


Figure 2: Test tank setup: cable responses were tested midwater and against fine and coarse sediment backgrounds.

The wideband signals used in these experiments are short duration bio-inspired pulses comprising pairs of downchirps. We use a set of six signals labeled DC1–DC6 in which only the rates of change of frequency of the constituent chirps differ. As previously reported these allow us to mimic much of the spectral variation seen in signals recorded from live dolphins performing target detection and localisation tasks [4].

## II. CABLE RESPONSES

Covering all experiments, around 10000 target echo measurements have been gathered. Responses have been measured for a range of cable aspects with consistent results seen to better than  $\pm 15^\circ$ . Beyond  $\pm 10^\circ$  the higher frequencies are lost progressively due to the frequency-dependent nature of the transducer beamwidths. Only a small fraction of the returns are presented here, but are typical of the characteristic broadside signatures strongly evident across the whole dataset. Data have been gathered midwater for three cable types and for other thin cylindrical objects of comparable dimensions to test discrimination capability. Further experiments have been directed to detection of cables lying on the concrete tank floor and on fine sand and coarse sediments.

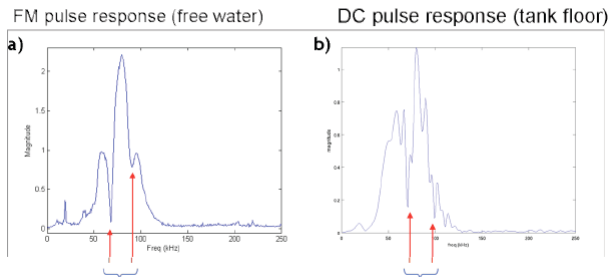


Figure 3: Cable responses: (a) free water, linear FM pulse; (b) biomimetic DC pulse, cable lying on tank floor. Red arrows indicate predictions for locations of key spectral notches

### A. Cable Models

Figure 3 shows two measured spectral responses for a type C cable using two different wideband pulses. The first spectrum is measured for the cable in free water, the second with the cable lying against the concrete tank floor. The red arrows indicate predicted positions for spectral notches derived from a cable model which considers only contributions from the specular reflection and a second wave formed from the propagation of the acoustic wave around an inner metallic layer.

This model is based on scattering theory for thin cylindrical shells. Since the outer plastic sheath has relatively low impedance (close to that of the surrounding water) some sound is reflected at this layer, but much of the energy is transmitted through the material to the relatively high impedance copper layer. Sound enters into this layer at the critical angle  $\theta_c$ , propagates around the metallic shell and is back-diffracted at the same angle  $\theta_c$ . These phenomena are the Lamb waves first described for acoustic propagation in thin plates and illustrated for the cylindrical shell example in Figure 4 .

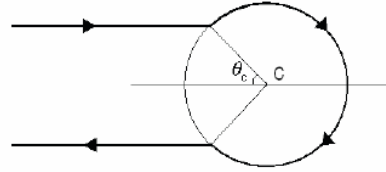


Figure 4: Lamb wave propagation path in cylindrical cross-section

Resolution of the wave equation for the thin plate allows us to calculate the speed of the Lamb waves and therefore estimate the delay between the main echo components [5, 6]. There are typically two Lamb wave modes, labelled  $S_0$ , symmetric, and  $A_0$ , anti-symmetric. At the frequencies of interest here the  $A_0$  wave is subsonic and only the  $S_0$  need be considered. Moreover, the  $S_0$  phase velocities are constant across the band and so the propagation in this layer is non-dispersive. The delay between the specular and secondary echoes depends on the relative velocities of the wavefronts propagating in the water and the copper layer, eqn. (1),

$$\Delta t_n = 2r \left( \frac{n\pi - \theta_c}{v_g} - \frac{1 - \cos \theta_c}{c} \right) \quad (1)$$

Note that  $n$  represents the number of turns around the cylinder and  $r$  is the radius of the copper layer. For the type C cable we arrive at:  $\Delta t_1 = 21 \mu\text{s}$  and  $\Delta t_2 = 43 \mu\text{s}$ . The empirically measured notch spacings are around 23kHz, equivalent to a time delay of  $43.8 \mu\text{s}$  and correspond well with the predicted  $\Delta t_2$  value.

### B. Cable Discrimination and Pulse Type

In these experiments, the cables are positioned at 1.5m range from the sonar, midwater at a depth of 0.8m. Spectral responses are given for the range of double chirp pulses showing that identification

can be achieved more readily using some pulses than others. In each case the responses have been normalized, since it is the shape rather than size of the response we are most interested in for discrimination. Given the nature of the tracking problem and the consistency of echoes over a  $\pm 10^\circ$  sector, all responses are measured at broadside aspect only.

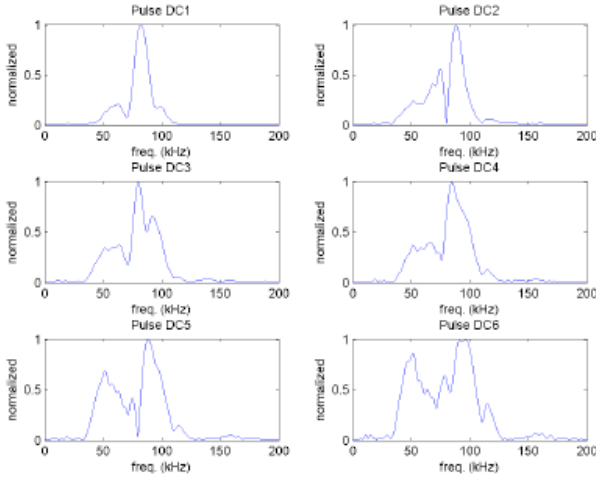


Figure 5: Spectral responses for cable type A, pulses DC1-DC6

Figure 5 gives the responses for cable type A, a 21mm diameter polyethylene sheathed cable. The variation seen between pulse types is in part due to the spectral shape of the pulse and in part due to the echo spectral response itself. Figure 6 shows the responses for the narrow (16.5mm Ø) type B cable. Here contributions from the ring of strengthening cables surrounding the conducting core typically give rise to more oscillatory spectral responses. In Figure 7, the responses to DC1 and DC2 for the larger 32mm diameter type C cable are similar to those for the type A cable. With more separation between the constituent chirps, using signals DC3-DC6, the responses are more varied. DC5 provides a good candidate for discrimination given the strong oscillations in the 50-80kHz band.

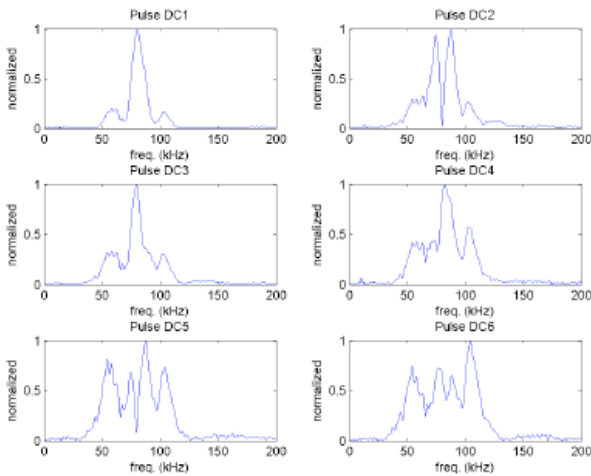


Figure 6: Spectral responses for cable type B, pulses DC1-DC6

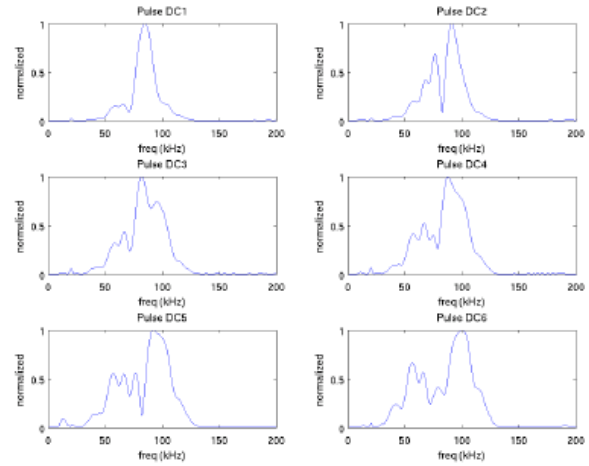


Figure 7: Spectral responses for cable type C, pulses DC1-DC6

Cable type D presents another distinctive set of responses to the six DC pulses, see Figure 8. In midwater consistency between pings is very good, but this cable response does have the lowest SNR as indicated by the relatively higher noise levels towards the 200kHz end of the spectra.

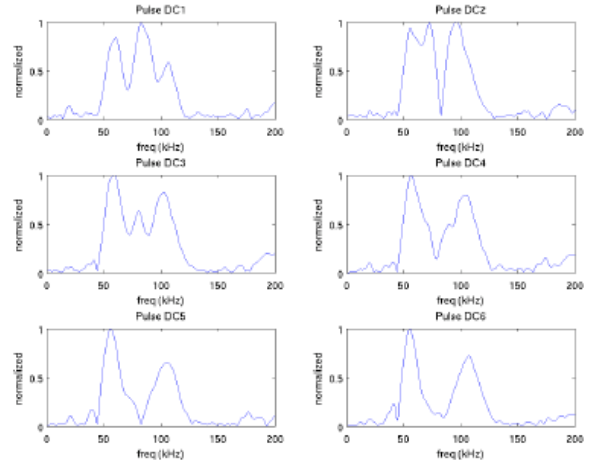


Figure 8: Spectral responses for cable type D, pulses DC1-DC6

### C. Discrimination of Cables from Similar Targets

To test discrimination between cables and alternative cylindrical targets with similar dimensions, we have also gathered data for sections of water-filled aluminium pipe (29mm ext. Ø) and an air-filled PVC tube (26mm ext. Ø). When water-filled, the PVC tube is strongly resonant and presents no difficulty in identification from its wideband response. Figure 9 gives responses for the three targets to pulses DC1 and DC3. Whilst the former gives an excellent SNR for detection, there is little discriminatory potential between the responses for the cable and the strong specular response of the air-filled PVC tube. Signal DC3 provides more energy around the notch seen in the cable response at 65kHz,

so the resulting notch in the echo spectrum using DC3 becomes a useful discriminatory feature. Note that as well as similar dimensions these all have similar target strengths. It is highly unlikely they could be distinguished using a conventional imaging sonar.

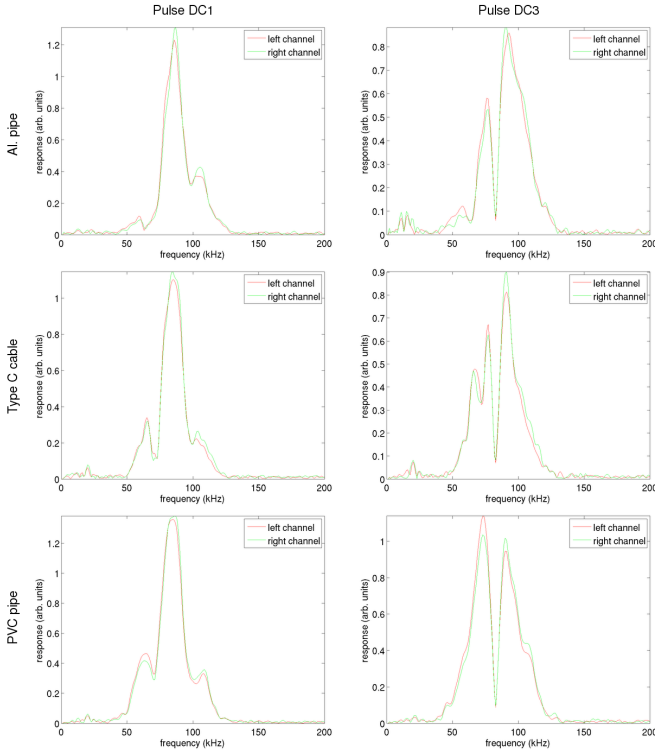


Figure 9: DC1 and DC3 target echo spectra for the type C cable and two similar scale cylindrical targets

### III. REVERBERATION IMPACT

To assess the impact of differences in seabed reverberation, cable responses were measured against very fine sand and coarse sand/grit sediments, with particle sizes varying from around 0.4mm to more than 4mm. The coarser sediment presents more difficulty for detection due to increased reverberation level which can be directly related to the bottom scattering strength through the following equation [7],

$$RL = SL - 2TL + S_v + 10 \log \frac{cT}{2} \psi r^2 \quad (2)$$

Figure 10 displays the bottom scattering strength calculated using APL-UW models for three different seabed types (very fine sand, sandy gravel and rough rock) relative to grazing angle [8]. This figure illustrates two important points for the detection process. Firstly, the rougher the sediment, the higher the reverberation level. The fine sand has a considerably lower bottom scattering strength than the coarse sand. Secondly, the grazing angle plays an important role in determining the reverberation noise level. For rough sediments, a lower grazing angle will provide better results.

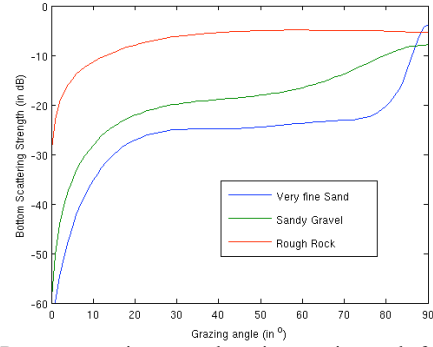


Figure 10: Bottom scattering strength against grazing angle for three seabed types – APL-UW models

Here we consider only our worst case with the low SNR type D cable lying on the coarse sediment. At 45° grazing angle the cable response is completely buried in reverberation noise at the beam centre presenting an extremely difficult task for detection and identification. In fact, better results are obtained by making use of the wide beam pattern and looking at the periphery of the beam, in effect using a shallower grazing angle. Figure 11 shows such a response to a DC4 pulse with the cable echo arrowed. Figure 12 presents the spectra for each of the six double chirp pulses. Though SNR is relatively low and the target response is well below the main lobe reverberation, the spectra do follow the general pattern of the responses measured midwater. Improved post-detection filtering and noise suppression would be of benefit in classifying these returns.

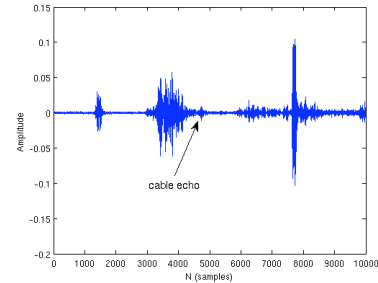


Figure 11: DC4 record at 45° grazing angle over coarse sand – cable echo is arrowed

At the 27° grazing angle we can use the main lobe returns without losing the cable echo in reverberation noise. Figure 13 gives spectra for the shallower grazing angle and the match with the midwater measurements is better. Finally we illustrate the variability in response over the coarse sediment by plotting a sequence of 43 DC3 echoes recorded at 5cm intervals along a 2m cable segment. In addition to the sediment reverberation, these data are compromised by cable curvature, tank wall returns, disturbances in the sediment surface and ambient noise sources. Figure 14 presents a waterfall plot of the cable echo spectra.

### IV. CABLE TRACKING

The responses above provide good discrimination capability but we do not rely on individual responses. More robust recognition and therefore improved tracking is achieved by integrating returns over series of pings to determine the most

likely track to follow. For open water trials on board a REMUS-100 AUV, the wideband system will be interfaced to the proven Autotracker framework [9,10], an embedded control architecture which uses detections from the sensor data to maintain vehicle track on the cable of interest.

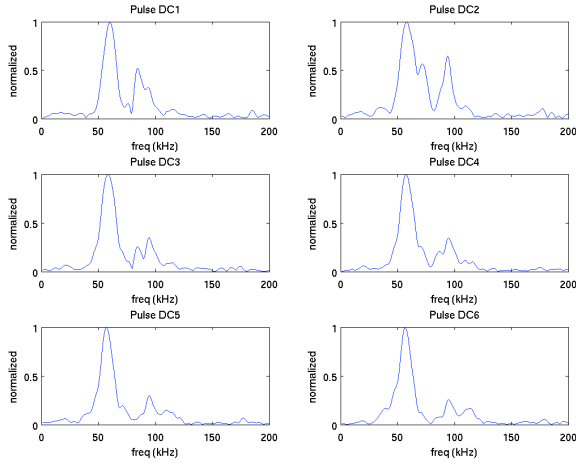


Figure 12: Spectral responses for the type D cable on coarse sand

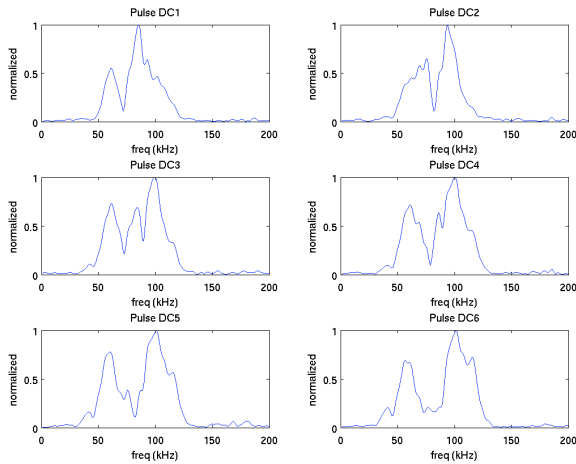


Figure 13: Spectral responses for the type D cable on coarse sand, 27° grazing angle, DC1-DC6

## V. BURIED OBJECTS

Wideband responses can help to distinguish material types. Though they are both smooth walled cylinders with similar dimensions and target strengths steel and PVC pipe responses are readily distinguished (Fig 15). We can therefore use different pulses to focus on parts of the spectrum that are of particular interest. This can greatly improve performance of classification methods and may explain variations seen in pulses transmitted by dolphins performing similar tasks.

At the frequencies used by the wideband sonar, we can expect some response from buried targets (Figure 16), and the challenge is to then be able to classify from a known midwater response. For a range of cylinder targets under test the

characteristic notch spacings are well preserved, though precise notch locations shift with burial. Careful choice of spectral features is needed to maintain classification performance

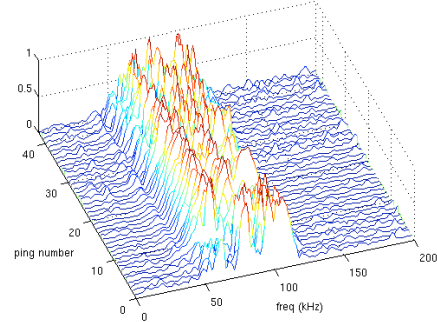


Figure 14: Waterfall plot of successive echo spectra at 5cm intervals tracking along cable on coarse sand – characteristic three-lobed DC3 echo for this cable is strongly evident

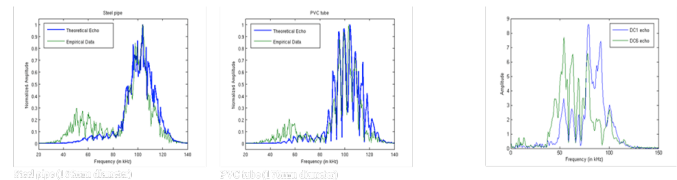


Figure 15: Modelled (blue) and measured (green) broadband echo responses from different materials

The concept of spectral texture can be useful for finding a way to track variations in responses for different targets through changes in aspect. We have adapted Haralick’s co-occurrence feature sets, originally conceived as image texture descriptors, to serve as measures for spectral texture. The feature values are calculated from normalized, quantized spectra and so throw away response amplitude information which is so important in recognition models based on image intensity data. We are more interested in detailed variations in spectral content than overall magnitude of response.

To track changes in feature values through variations in target aspect, we use a hidden Markov model. This requires the specification of transition probabilities ( $a_{ij}$ ) between states and emission probabilities ( $b_{jk}$ ), the probability of observing a particular feature value given some object state. In this case a state corresponds to a particular target lying at a particular aspect with respect to the sonar.

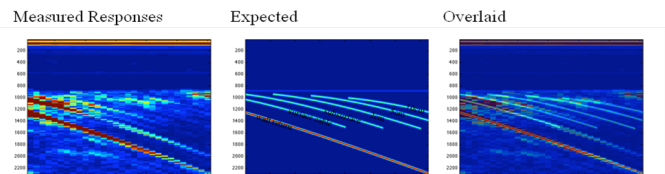


Figure 16: Detections for small diameter (24mm) plastic sheathed cables buried at various depths in fine sand sediment. Highly reverberant

For robust classification the HMM integrates returns over a range of target aspects, as would be seen in an autonomous underwater vehicle (AUV) transit past a target lying on the

seabed. In addition, these feature sets show some evidence of capacity for generalization. After receiving just one wideband target echo, we are able to see similarities in response between smooth manmade objects or between rougher objects, eg. Rocks and concrete blocks. After 10 pings have been received objects can be firmly identified and their aspect can be accurately estimated (Fig 17)

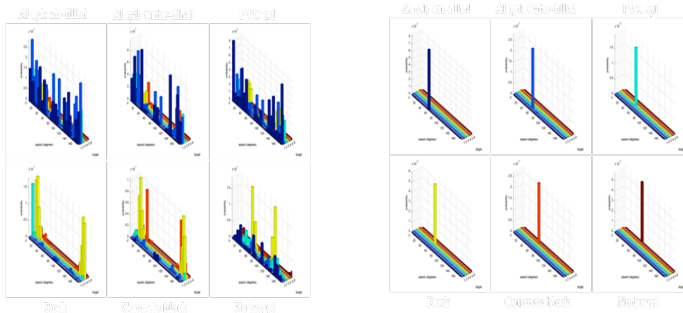


Fig 17: Left: After one ping, similar objects have similar responses, aspect cannot be determined  
Right: After ten pings, object and aspect are correctly identified.

## VI. CONCLUSIONS

This study has demonstrated the capability of the wideband bio-inspired sonar system to distinguish between different cable types, laying down the groundwork for the automated tracking of small communications cables underwater. In summary, we have demonstrated that cables give a consistent, measurable and discriminatory response to the wideband pulses. We have noted that over more reverberant surfaces a shallower grazing angle is required to maintain good SNR. The wide beamwidth of the sensors ensures good detection over a wide range of aspects ( $\pm 20^\circ$ ).

For object classification and buried object detection we have observed that:

- The wideband sonar is highly effective in classification and recognition of midwater and bottom set targets from characteristic ‘broadside’ responses. In particular:
- Using spectral texture features and an HMM classifier, this performance can be extended to classification of targets lying at any aspect with circa  $25^\circ$  of data required to make classification decision
- Buried and partially buried targets can be identified if features are carefully selected
- Small diameter cables, can be detected at burial depths of around 10cm. Response is less well suited to identification given very low SNR

## ACKNOWLEDGEMENTS

This research programme is supported by the US Naval Facilities and Engineering Command (NAVFAC).

## REFERENCES

- [1] W. W. L. Au. *The Sonar of Dolphins*. Springer-Verlag, New York, 1993.
- [2] D. A. Helweg, P. W. Moore, S. W. Martin, and L. A. Dankiewicz. Using a binaural biomimetic array to identify bottom objects ensounded by echolocating dolphins. *Inst. Phys. Bioinspiration & Biomimetics*, 1(2): pp. 41–51, June 2006.
- [3] C. Capus, Y. Pailhas, and K. Brown. Wideband sonar system for autonomous surveys using REMUS. *In J. Acoust. Soc. Am.*, vol. 123(5) Pt. 2, p. 3466, May 2008.
- [4] C. Capus, Y. Pailhas, K. Brown, D. M. Lane, P.W. Moore, and D. Houser. Bio-inspired wideband sonar signals based on observations of the bottlenose dolphin (*Tursiops truncatus*). *J. Acoust. Soc. Am.*, 121(1): pp. 594–604, January 2007.
- [5] P. L. Marston. GTD for backscattering from elastic spheres and cylinders in water, and coupling of surface elastic waves with the acoustic field. *J. Acoust. Soc. Am.*, 83(1): pp. 25–37, January 1988.
- [6] S. G. Kargl and P. L. Marston. Observations and modelling of the backscattering of short tone bursts from a spherical shell: Lamb wave echoes, glory, and axial reverberations. *J. Acoust. Soc. Am.*, 85(3): pp. 1014–1028, March 1989.
- [7] R. J. Urlick. *Principles of Underwater Sound*. Peninsula, Los Altos, CA, 3 edition, 1983.
- [8] APL-UW. *High Frequency Ocean Environmental Acoustic Models Handbook*. Tech. Report APL-UW TR 9407, Applied Physics Laboratory, University of Washington, Seattle, WA, USA, October 1994.
- [9] J. Evans, Y. Petillot, P. Redmond, M. Wilson, and D. M. Lane. AUTOTRACKER: AUV embedded control architecture for autonomous pipeline and cable tracking. *In IEEE Oceans 2003*, pp. 2651–2658, San Diego, CA, September 2003.
- [10] P. Patron, J. Evans, J. Brydon, and J. Jamieson. AUTOTRACKER: autonomous pipeline inspection: sea trials 2005. *In World Maritime Technology Conference – Advances in Technology for Underwater Vehicles*, London, March 2006.